AJNR

Angiogenesis and Blood-Brain Barrier Breakdown Modulate CT Contrast Enhancement: An Experimental Study in a Rabbit Brain-Tumor Model

David Zagzag, Marvin Goldenberg and Steven Brem

AJNR Am J Neuroradiol 1989, 10 (3) 529-534
http://www.ajnr.org/content/10/3/529

Angiogenesis and Blood-Brain Barrier Breakdown Modulate CT Contrast Enhancement:

An Experimental Study in a Rabbit Brain-Tumor Model

David Zagzag[1-3]
Marvin Goldenberg[4]
Steven Brem[1,2]

Because of the crucial role played by tumor neovascularization in contrast enhancement, we studied the CT imaging findings in a transplantable rabbit brain tumor, the VX2 carcinoma that induces angiogenesis and the breakdown of blood-brain barrier associated with contrast enhancement. Tumor detection by contrast enhancement followed the peak of angiogenesis. Inhibition of angiogenesis, by copper depletion and penicillamine, led to avascular tumors that lack contrast enhancement. Furthermore, there was no contrast enhancement in brain adjacent to the tumor of normocupremic rabbits or within the hypocupremic tumor, despite the breakdown of the blood-brain barrier, without the concomitant presence of angiogenesis.

We conclude that contrast enhancement of intracranial tumors is dependent primarily on the proliferation of the microvasculature.

Contrast enhancement is one of the main radiologic manifestations of CNS tumors; it is not observed, however, in all tumors [1]. The mechanisms that cause the contrast enhancement of brain tumors are not entirely known but remain important to the interpretation of CT scans. These mechanisms relate to breakdown of the blood-brain barrier (BBB) [2–5] and to tumor neovascularization, that is, angiogenesis [6–12]. The growth of tumors outside the CNS [13] and in the brain [14, 15] proceeds through two stages: the early avascular and the later vascular phases. Prevention of angiogenesis arrests tumor growth at the avascular stage [16]. Tumor neovascularization is prevented in the cornea [17, 18] and in the brain [19] by the depletion of copper, a necessary cofactor for angiogenesis [17, 20].

The present study was designed to investigate the mechanisms that modulate contrast enhancement. We selected the rabbit VX2 carcinoma, useful for radiologic research [21–23], studies of BBB, and angiogenesis [24]. We compared the serial CT images, extravasation of Evans blue, and histology of normocupremic and hypocupremic tumors.

Materials and Methods

We implanted 5×10^5 cells of the VX2 carcinoma into the right parietal lobe of 36 3-kg male New Zealand white rabbits, according to a model of intracerebral angiogenesis and tumor growth [24].

We divided the rabbits into six groups of six animals each: four for CT imaging and two for study of the BBB. Tumor size and histology were determined in each of the six animals. Groups 1–5 were fed a normal diet* throughout the experiment. Group 6 animals were fed a low-copper diet,† beginning 6 weeks before tumor implantation, and given 20 mg of D-penicillamine‡ per os, thrice daily, 6 days before and after tumor-cell implantation [17].

CT studies were performed on an Elscint Exel 2002, with the following settings: circle diameter, 140 mm; X-ray current, 40 mA; voltage, 140 kV; scan time, 10.5 sec; slice width, 3 mm; and image matrix, 340 × 340. The brains of the rabbits were imaged in the coronal and axial planes before and 5 min after completion of IV administration of 3 ml/kg of iothalamate meglumine§ given as a bolus.

* #5301, Ralston Purina Canada Inc., Longueuil, Quebec.
† #5890C-1, Ralston Purina, Richmond, IN.
‡ #4875, Sigma Chemical Co., St. Louis, MO.
§ Conray 60, Mallinckrodt Laboratories, Pointe-Claire, Quebec, Canada.

This article appears in the May/June 1989 issue of *AJNR* and the July 1989 issue of *AJR*.

Received February 17, 1988; accepted after revision October 25, 1988.

This work was supported in part by grant MA-8672 from the Medical Research Council of Canada.

D. Zagzag is supported by a Postdoctoral Fellowship grant from the Cancer Research Society, Inc.

[1] Department of Neurosciences, Sir Mortimer B. Davis–Jewish General Hospital, 3755 Cote Ste. Catherine, Suite C-130, Montreal, Quebec H3T 1E2, Canada. Address reprint requests to S. Brem.

[2] Department of Neurology and Neurosurgery, McGill University School of Medicine, Montreal, Quebec H3T 1E2, Canada.

[3] Present address: Department of Pathology, New York University Medical Center, 550 First Ave., New York, NY 10016.

[4] Department of Radiology, Sir Mortimer B. Davis–Jewish General Hospital and McGill University School of Medicine, Montreal, Quebec H3T 1E2, Canada.

***AJNR* 10:529–534, May/June 1989**
0195–6108/89/1003–0529

Group 1 was scanned 6 days after implantation, and immediately sacrificed. Groups 2–5 were likewise studied and sacrificed on days 10, 14, 18, and 22, respectively. In group 6, a CT scan was obtained only when the animals developed neurologic deterioration (gait disturbances, decreased level of consciousness). The brains were removed and fixed in 10% phosphate-buffered formalin for 6 days. The specimens were sectioned coronally at 1.5-mm intervals and correlated to the CT coronal scans.

One hour before sacrifice, two rabbits in each group received 2% Evans blue (2 ml/kg) injected IV via the marginal vein of the ear. The brains were then removed and evaluated for Evans blue extravasation by using a semiquantitative scale [25].

After fixation and coronal sections, tumor volume was determined by measuring coronal (d1), axial (d2), and transverse (d3) diameters using the formula $(d1 \times d2 \times d3 \times \pi)/6$ [26]. The specimens were then examined histologically. Tumor neovascularization was scored by using a histologic method that computes microvascular density, endothelial hyperplasia, and endothelial cytology [27]. Vascular density was defined in our study as the number of microvessels per field (×200).

Blood samples were taken in all the animals at the beginning of the experiment, at time of surgery, and at time of sacrifice for serum copper determinations [28].

Statistical analysis of tumor volume was performed by analysis of variance and Tukey test [29]. A $p < .05$ was the chosen level for significance.

Results

Serum copper levels are shown in Table 1. Groups 1–5 were normocupremic throughout the experiment, whereas group 6 was hypocupremic at the time of tumor-cell implantation and sacrifice. The mean survival time in group 6 was 19 ± 1.8 days.

CT Findings

In the normocupremic animals, there was no tumor detection at any time without contrast infusion. Even with contrast infusion, there was still no visualization of the tumor on days 6 and 10. Starting at day 14, the tumor first showed dense, round, homogeneous, well-defined enhancement (Fig. 1A). As the tumor enlarged, it became more oval on day 18 (Fig. 2A).

TABLE 1: Serum Copper Levels in Rabbits Implanted with Tumor

Group No.	Day of Sacrifice	No. of Rabbits	Copper Level (μg/dl)		
			Start	Day of Tumor Implantation	Day of Sacrifice
1	6	6	73.3 ± 10.3	62.4 ± 9.9	62.1 ± 9.4
2	10	6	70.0 ± 10.2	61.1 ± 9.5	60.6 ± 8.9
3	14	6	57.0 ± 10.6	62.9 ± 8.2	59.2 ± 9.8
4	18	6	62.2 ± 11.5	64.6 ± 3.9	63.8 ± 15.2
5	22	5[a]	61.8 ± 8.8	61.3 ± 4.2	63.7 ± 9.3
6	19 ± 1.8	6	69.5 ± 12.8	11.9 ± 3.6	7.4 ± 4.4

Note.—Groups 1–5 were fed a normal diet; group 6 was fed a low-copper diet.

[a] Sixth animal excluded because of death before scheduled CT.

Finally, on day 22, patchy areas of decreased attenuation appeared within the center of the tumor (Fig. 3A). The lesion itself remained very well defined at all times. CT was not performed in one animal in group 5 because it died before day 22. The tumor was visualized with CT in all the other normocupremic rabbits studied on days 14, 18, and 22.

CT in the hypocupremic animals appeared normal even after injection of contrast material (Fig. 4A). In both normo- and hypocupremic groups we failed to observe peritumoral edema.

Histologic Findings

In normocupremic tumors, a slight capillary proliferation first appeared on day 6. The vascular density increased progressively until day 14, when neovascularization was prominent (Fig. 1B). On day 18, tumor vascularity was slightly decreased (Fig. 2B). By day 22, vascularized tumors accompanied by central necrosis were present in all normocupremic rabbits (Fig. 3B). The cortical surface revealed many enlarged tortuous peritumoral vessels resembling those of human malignant tumors [30]. The progression of volume and vascular density in the normocupremic tumor is summarized in Table 2 and Figure 5.

The tumors in the hypocupremic groups were tiny, pale, laminar plaques with 91% less volume compared with the normocupremic tumors on day 22 (Table 2). The cortical surface of hypocupremic rabbits showed a normal vascular pattern. Microscopically, the tumor cells retained malignant features and appeared viable, but the capillary density was close to that of a normal brain, indicating that angiogenesis failed to occur (Fig. 4B).

Evans Blue Studies

In normocupremic animals (groups 1–5) Evans blue extravasation appeared in the tumor area by day 6 and around the tumor by day 14. Extravasation was not seen on the cortical surface on day 14 (Fig. 1C). By day 18 extravasation was prominent in the tumor and brain adjacent to tumor and was detected on the cortical surface (Fig. 2C). Finally, by day 22, we observed severe extravasation in the tumor and at the level of the cortical surface (Fig. 3C). The hypocupremic animals in group 6 revealed marked extravasation in and around the tumor (Fig. 4C).

In summary (Table 2), in normocupremic rabbits, contrast enhancement allowing tumor detection was possible only when angiogenesis was prominent by day 14. In the hypocupremic rabbits, even though the tumor volume at the time of sacrifice was larger (46.8 ± 26.6 mm^3) than the tumor volume on day 14 (13.2 ± 2.2 mm^3) in normocupremic rabbits, no tumor was visualized on CT, even after contrast injection. Evans blue extravasation was observed in normocupremic tumors at all stages and around them on day 14; in hypocupremic tumors Evans blue extravasation was noted in and around the tumor.

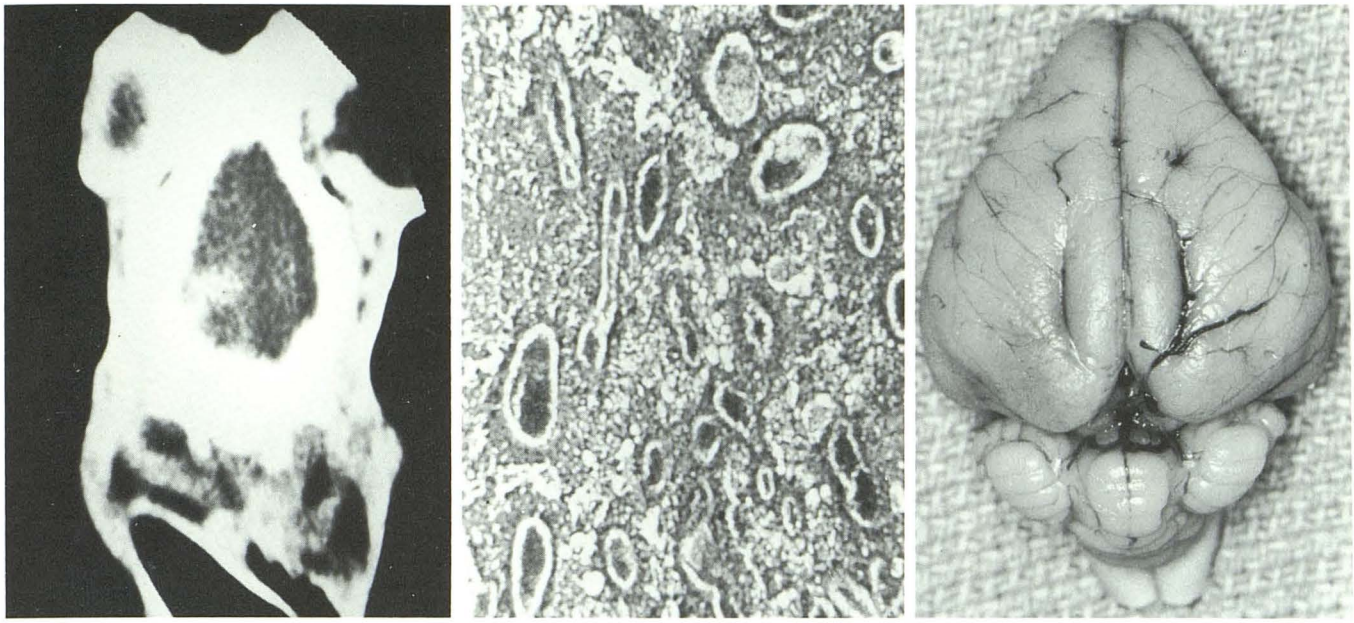

A B C

Fig. 1.—Normocupremic tumor on day 14.
A, Axial CT scan shows enhancing tumor nodule of right high convexity.
B, Highly vascularized tumor. (H and E, ×200)
C, Cortical surface fails to reveal Evans blue extravasation on day 14.

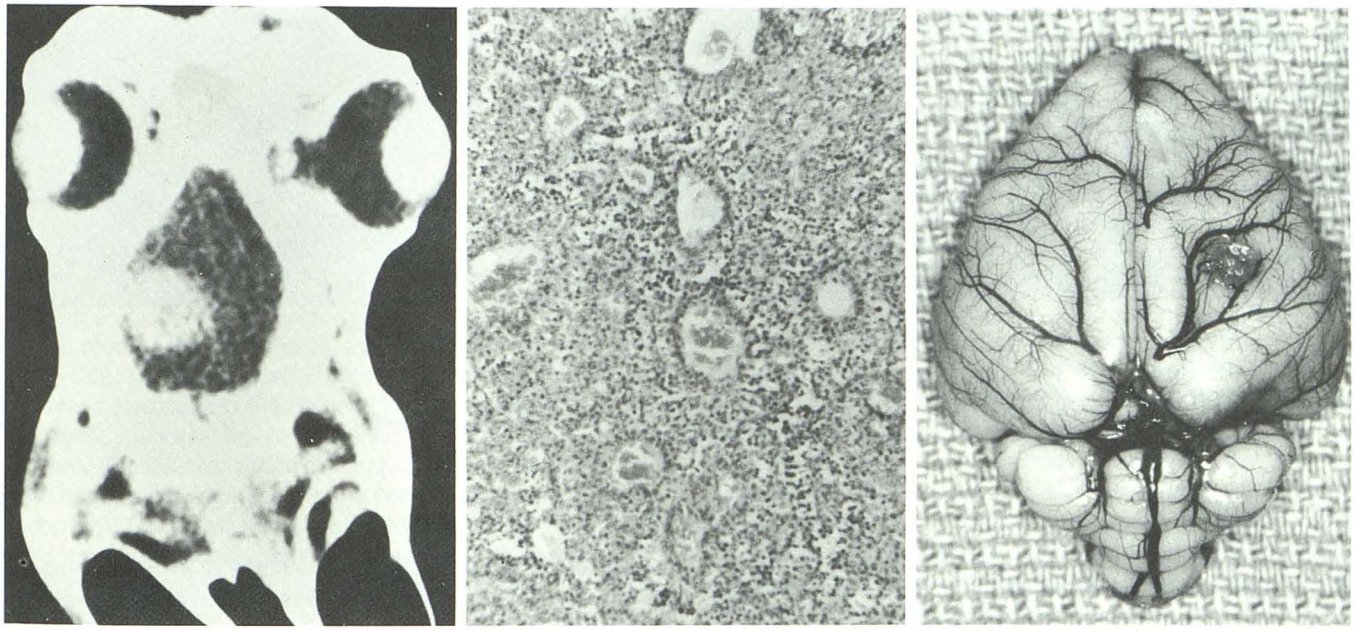

A B C

Fig. 2.—Normocupremic tumor on day 18.
A, Axial CT scan shows large homogeneously enhancing tumor on right.
B, Slight decrease of tumor vascular density. (H and E, ×250)
C, Cortical surface reveals localized area of Evans blue extravasation.

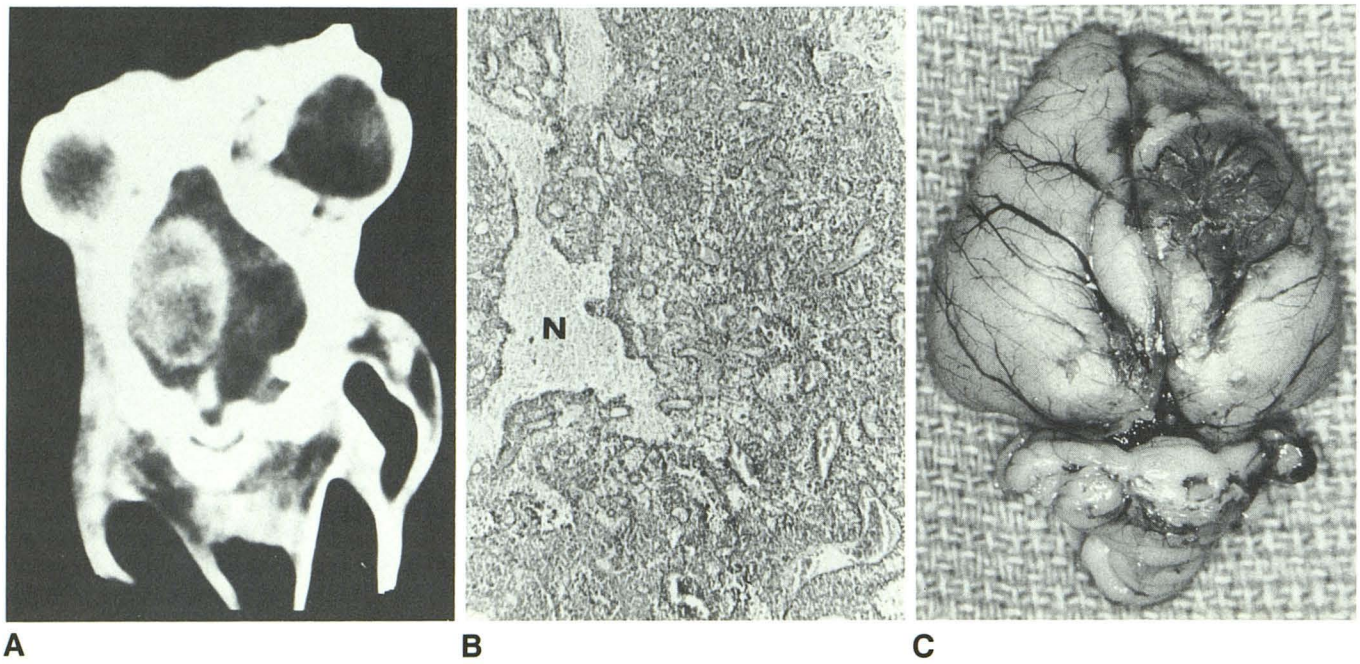

Fig. 3.—Normocupremic tumor on day 22.
A, Axial CT scan reveals further enlargement of tumor, but now with some inhomogeneity and areas of decreased attenuation corresponding to tumor necrosis.
B, Prominent vascular proliferation at tumor periphery around central necrosis (N). (H and E, ×150)
C, Severe Evans blue extravasation seen on cortical surface on day 22.

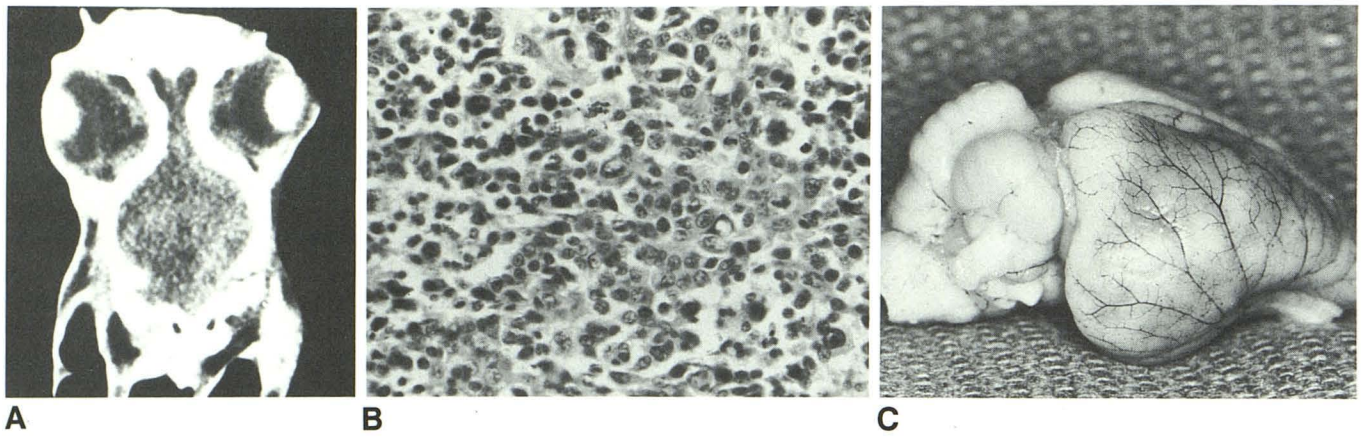

Fig. 4.—Hypocupremic tumor.
A, Axial CT scan. No contrast enhancement is detected.
B, Light microscopy reveals lack of vascular proliferation in tumor; angiogenesis is suppressed. (H and E, ×450)
C, Broad areas of Evans blue extravasation are observed on cortical surface around tumor.

In normocupremic animals, on day 18, we observed necrosis and punctate hemorrhages with light microscopy, but not by CT scanning. Necrosis was observed on CT on day 22 when it was more prominent by histopathology.

Discussion

Currently, two interrelated mechanisms are invoked to explain the contrast enhancement of tumors on CT: (1) breakdown of the BBB with passage of iodine across the basement membrane of the capillaries into the tumor [2–5] and (2) tumor neovascularization leading to increased intravascular levels of iodine [6–12], that is, "computed angiotomography" [8], with a positive correlation between contrast enhancement and the degree of vascularity [7]. Because of the newly discovered ability to pharmacologically suppress capillary growth induced by brain tumors [18, 19], we could test the relative contributions of BBB breakdown and angiogenesis.

The exact mechanism by which copper regulates angiogenesis is unknown [31], but the following observations link

TABLE 2: Tumor Vascularity, Size, Breakdown of the Blood-Brain Barrier (BBB), and Contrast Enhancement in Rabbits Implanted with Tumor

Group	Day of CT and Sacrifice	No. of Rabbits	Tumor Vascularity[a]	Tumor Size (mm^3)	Breakdown of BBB[b]		Contrast Enhancement	
					Tumor	BAT	Tumor	BAT
Normocupremic								
1	6	6	5.2 ± 1.0	0.2 ± 0.04	+	0	No	No
2	10	6	8.7 ± 1.5	0.7 ± 0.2	+	0	No	No
3	14	6	16.5 ± 1.6	13.2 ± 2.2	++	+	Yes	No
4	18	6	13.7 ± 1.4	70.0 ± 17.5	++	++	Yes	No
5	22	5[c]	12.4 ± 1.5	513.5 ± 128.0	+++	++	Yes	No
Hypocupremic								
6	19.5 ± 1.8	6	4.2 ± 0.8	46.8[d] ± 26.6	+++	++	No	No

Note.—All data expressed represent mean ± SD. BAT = brain adjacent to tumor.

[a] Number of microvessels per field. (×200)

[b] Breakdown of BBB detected by extravasation of Evans blue: 0 = none; + = slight; ++ = moderate; +++ = severe.

[c] Sixth animal excluded from the study because of death caused by tumor growth before scheduled day of CT.

[d] Statistically significant difference from normocupremic tumors on day 22 ($p < .01$).

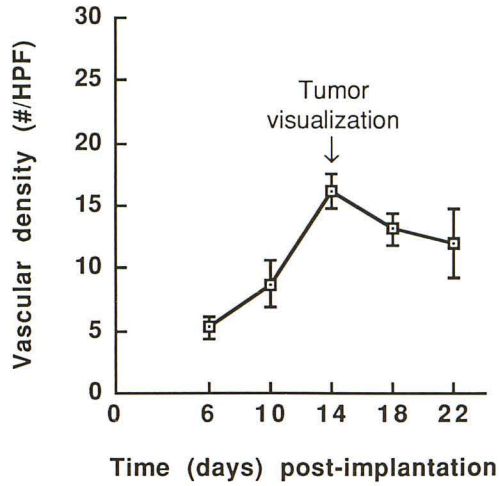

Fig. 5.—Progression of vascular density in normocupremic animals. CT tumor visualization correlates with peak tumoral angiogenesis. HPF = high-power field.

TABLE 3: Angiogenesis and Breakdown of the Blood-Brain Barrier as Causes of Contrast Enhancement in Tumor-Implanted Rabbits

Group	Angiogenesis	Breakdown of Blood-Brain Barrier[a]	Contrast Enhancement
Normocupremic			
Tumor	+	+	+
Brain adjacent to tumor	−	+	−
Hypocupremic			
Tumor	−	+	−
Brain adjacent to tumor	−	+	−

[a] Detected by Evans blue extravasation.

copper as a cofactor for angiogenesis: (1) copper ion, but not other metal salts, stimulates endothelial cell locomotion in vitro [32]; (2) a local rise of copper concentration precedes neovascularization in the cornea [17]; (3) copper salts act in a dose-dependent fashion as a chemoattractant to induce corneal neovascularization in vivo [33]; and (4) ceruloplasmin and heparin are angiogenic in the cornea only when bound to copper [20]. Penicillamine, a chelator of copper, contributes to copper depletion by acceleration of copper clearance [17].

Contrast enhancement appeared on day 14 in normocupremic tumors and failed to appear in larger hypocupremic tumors (Table 2), excluding size alone as a determinant of contrast enhancement. In the hypocupremic group, the Evans blue extravasation revealed the breakdown of the BBB, both within the tumor and in the peritumoral area. CT scans of hypocupremic animals, however, failed to reveal enhancement after iothalamate meglumine injection. In hypocupremic tumors, angiogenic inhibition likely prevented contrast enhancement. On the other hand, contrast enhancement appeared in normocupremic malignant tumors that contain numerous new blood vessels.

The permeability of newly formed capillary sprouts compared with that of mature capillaries is increased [34]. Normal capillaries of the brain maintain the integrity of the BBB [35], but the blood vessels of experimental [36] and human [37] brain tumors are structurally altered and have an increased capillary permeability. In normocupremic rabbits, the presence of both tumor angiogenesis and breakdown of the BBB is linked to the appearance of contrast enhancement. In hypocupremic rabbits, however, the breakdown of the BBB is not sufficient by itself to result in contrast enhancement.

Evans blue binds to albumin and has a molecular weight of 68,500 daltons [38], whereas iothalamate meglumine has a molecular weight of 800 daltons. Comparison of molecular weights does not explain the leakage of Evans blue and the failure of contrast material to cross an open BBB. To explain the paradox between the appearance of Evans blue extravasation and the absence of contrast enhancement, we suggest that the interval after injection of iothalamate, 5 min, compared with the longer interval after injection of Evans blue, 1 hr, accounts for the appearance of Evans blue extravasation, despite the greater molecular weight of Evans blue. It is plausible that if the CT scans were obtained 1 hr after

the injection of iothalamate, the hypocupremic tumors might have shown contrast enhancement. Our data support the concept that if a CT scan is obtained immediately after injection, the contrast enhancement probably correlates with vascularity [7].

There was a correlation between the histologic boundary of the tumors and contrast enhancement in the normocupremic group. On day 22, at the periphery of the tumor, both vascularity [24] and contrast enhancement were prominent. The topographic distribution corresponds to the growth patterns of malignant human gliomas, where contrast enhancement and vascular proliferation are both conspicuous at the growing edge [10–12, 39]. The zone of Evans blue extravasation, however, did not correlate with histologic evidence of angiogenesis nor with the radiologic appearance of CT contrast enhancement.

We conclude from our data (Tables 2 and 3) that breakdown of the BBB was a necessary but not sufficient condition for contrast enhancement and that angiogenesis in our brain-tumor model was a key requirement for the appearance of contrast enhancement.

Angiogenesis occurs at the microvascular level. For clinical imaging, contrast enhancement in CT scanning is a sensitive guide to vascular proliferation and differs from angiography, which delineates the macrovessels or their branches.

ACKNOWLEDGMENTS

We thank Y. Tanaka for determinations of serum copper levels, Sylvano Ordonselli and Lynn Miller for technical assistance, Suzanne Wileman for photography, and A. S. Luck and M. Maritzer for typing the manuscript.

REFERENCES

1. Ambrose J, Gooding MR, Richardson AE. Sodium iothalamate as an aid to diagnosis of intracranial lesions by computerized transverse axial scanning. *Lancet* **1975**;2:669–674
2. Ambrose J. Computerized transverse axial scanning (tomography). Part 2. Clinical application. *Br J Radiol* **1973**;46:1023–1047
3. Gado MH, Phelps ME, Coleman RE. An extravascular component of contrast enhancement in cranial computed tomography. Part I: The tissue blood ratio of contrast enhancement. Part II: Contrast enhancement and the blood tissue barrier. *Radiology* **1975**;117:589–593, 595–597
4. Kormano M, Dean PB. Extravascular contrast material: the major component of contrast enhancement. *Radiology* **1976**;121:379–382
5. Britt RH, Lyons BE, Enzmann DR, Saxer EL, Bigner SH, Bigner DD. Correlation of neuropathological findings, computerized tomographic and high resolution ultrasound scans of canine avian sarcoma virus–induced brain tumors. *J Neurooncol* **1987**;4:243–268
6. Ethier R, Sherwin A, Taylor S, et al. Computerized angiotomography. The use of 100 cc of Hypaque M-60%, clinical and experimental results. Presented at the symposium on computerized axial tomography, Montreal, Quebec, Canada, May **1974**
7. Taveras JM, Wood EH. *Diagnostic neuroradiology*, vol. 2, 2nd ed., part IV. *Selection of diagnostic procedures*. Baltimore: Williams & Wilkins, **1976**:1000
8. Messina AV, Potts DG, Rottenberg D, Patterson RH. Computed tomography: demonstration of contrast medium within cystic tumors. *Radiology* **1976**;120:345–347
9. Butler AR, Horii SC, Kricheff II, Shannon MB, Budzilovich GN. Computed tomography in astrocytomas. A statistical analysis of the parameters of malignancy and the positive contrast-enhanced CT scan. *Radiology* **1978**;129:433–439
10. Daumas-Duport C, Meder JF, Monsaingeon V, Missir O, Aubin ML, Szikla G. Cerebral gliomas: malignancy, limits and spatial configuration. Comparative data from serial stereotaxic biopsies and computed tomography (a preliminary study based on 50 cases). *J Neuroradiol* **1983**;10:51–80
11. Zimmerman HM. The pathology of primary brain tumors. *Semin Roentgenol* **1984**;19:129–138
12. Kelly PJ, Daumas-Duport C, Kispert DB, Kall BA, Scheithauer BW, Illig JJ. Imaging based stereotaxic serial biopsies in untreated intracranial glial neoplasms. *J Neurosurg* **1987**;66:865–874
13. Folkman J. Tumor angiogenesis. *Adv Cancer Res* **1974**;19:331–348
14. Brem S. The role of vascular proliferation in the growth of brain tumors. *Clin Neurosurg* **1976**;23:440–453
15. Deane BR, Lantos PL. The vasculature of experimental brain tumors. Part 1: A sequential light and electron microscope study of angiogenesis. *J Neurol Sci* **1981**;49:55–66
16. Brem S, Brem H, Folkman J, et al. Prolonged tumor dormancy by prevention of neovascularization in the vitreous. *Cancer Res* **1976**;36:2807–2812
17. Ziche M, Jones J, Gullino PM. Role of prostaglandin E_1 and copper in angiogenesis. *JNCI* **1982**;69:475–482
18. Alpern-Elran H, Brem S. Angiogenesis in human brain tumors: inhibition by copper depletion. *Surg Forum* **1985**;36:498–500
19. Zagzag D, Brem S. Control of neoplastic development in the brain: copper depletion prevents neovascularization and tumor growth. *Surg Forum* **1986**;37:506–509
20. Raju KS, Alessandri G, Ziche M, Gullino PM. Ceruloplasmin, copper ions, and angiogenesis. *JNCI* **1982**;69:1183–1188
21. Carson BS, Anderson JH, Grossman SA, et al. Improved rabbit brain tumor model amenable to diagnostic radiographic procedures. *Neurosurgery* **1982**;11:603–608
22. Cochran ST, Higashida RT, Holburt E, Winter J, Iwamoto K, Norman A. Development of rabbit brain tumor model for radiologic research. *Invest Radiol* **1985**;20:928–932
23. Kumar AJ, Hassenbusch S, Rosenbaum AE, et al. Sequential computed tomographic imaging of a transplantable rabbit brain tumor. *Neuroradiology* **1986**;28:81–86
24. Zagzag D, Brem S, Robert F. Neovascularization and tumor growth in the rabbit brain: a model for experimental studies of angiogenesis and blood-brain barrier. *Am J Pathol* **1988**;131:361–372
25. Sage MR, Wilcox J, Evill CA, Benness GT. Comparison of blood-brain barrier disruption by intracarotid iopamidol and methylglucamine iothalamate. *AJNR* **1983**;4:893–895
26. Auerbach R, Morrissey LW, Sidky YA. Regional differences in the incidence and growth of mouse tumors following intradermal or subcutaneous inoculation. *Cancer Res* **1978**;38:1739–1744
27. Brem S, Cotran RS, Folkman J. Tumor angiogenesis: a quantitative method for histologic grading. *JNCI* **1972**;48:347–356
28. Yasuda K, Koizumi H, Ohishi K, Noda T. Zeeman effect atomic absorption. *Prog Anal Atomic Spectr* **1980**;3:299–368
29. Sokal RR, Rohlf FJ. *Biometry. The principles and practice of statistics in biological research*, 2nd ed. San Francisco: Freeman, **1981**:454–477
30. Nystrom S. Pathological changes in blood vessels of human glioblastoma multiforme. Comparative studies using plastic casting, angiography, light microscopy and electron microscopy, and with reference to some other brain tumors. *Acta Pathol Microbiol Scand [Suppl]* **1960**;49(137):1–83
31. Folkman J, Klagsbrun M. Angiogenic factors. *Science* **1987**;235:442–447
32. McAuslan BR, Reilly W. Endothelial cell phagokinesis in response to specific metal ions. *Exp Cell Res* **1980**;130:147–157
33. Parke A, Bhattacherjee P, Palmer RMJ, Lazarus NR. Characterization and quantification of copper sulfate induced vascularization of the rabbit cornea. *Am J Pathol* **1988**;130:173–178
34. Abell RG. The permeability of blood capillary sprouts and newly formed blood capillaries as compared to that of older blood capillaries. *Am J Physiol* **1946**;147:237–241
35. Goldstein GW, Betz AL. Recent advances in understanding brain capillary function. *Ann Neurol* **1983**;14:389–395
36. Nishio S, Ohta M, Abe M, et al. Microvascular abnormalities in ethylnitrosourea (ENU)-induced rat brain tumors: structural basis for altered blood brain barrier function. *Acta Neuropathol* (Berl) **1983**;59:1–10
37. Long DM. Capillary ultrastructure and the blood brain barrier in human malignant brain tumors. *J Neurosurg* **1970**;32:127–144
38. Neuwelt EA, Rapoport SI. Modification of the blood-brain barrier in the chemotherapy of malignant brain tumors. *Fed Proc* **1984**;43:214–219
39. Burger PC, Dubois PJ, Schold SC, et al. Computerized tomographic and pathologic studies of the untreated, quiescent, and recurrent glioblastoma multiforme. *J Neurosurg* **1983**;58:159–169